DRAFT
CMS Paper

The content of this note is intended for CMS internal use and distribution only

2022/10/20
Archive Hash: 2aa95d2-D
Archive Date: 2022/09/23

Search for exotic decays of the Standard Model Higgs boson to pseudoscalars in the high mass region, with a pair of muons and tau leptons in the final state with the full Run II Dataset

The CMS Collaboration

Abstract

A search is conducted for exotic decays of the Standard Model Higgs Boson, H, decaying to a pair of pseudoscalars, a, which then decay to a pair of muons and tau leptons. Pseudoscalar masses between 20 and 60 GeV are investigated using the full Run II dataset, corresponding to 137 fb^{-1}. Motivation for the existence of the pseudoscalar Higgs particle is primarily supported by Beyond Standard Model (BSM) Two Higgs Doublet Models with the extension of a Singlet (2HDM+S) theories - which include the Next to Minimal Super Symmetric Model (NMSSM). Upper limits on the branching fraction are set.

1 Introduction

With the discovery of the Higgs Boson in 2012 with the Run I dataset, physicists have entertained the idea of using the Higgs as a window for new physics. Due to the Nature of the Electroweak Symmetry Breaking Mechanism [1–6], the Higgs couples to all Standard Model particles. Beyond Standard Model (BSM) theories contain ample room for the Higgs to couple to particles beyond the SM, making the Higgs an excellent window to investigate any physics beyond the SM. In this paper, several well motivated BSM theories are considered. Noteably, the two Higgs doublet model (2HDM) with it's extension of a scalar singlet is considered (2HDM+S). These types of BSM theories can solve the μ coupling problem in Super Symmetry (SUSY), while maintaining general support of SUSY (Holomorphy), Axion-like Models (Peccei-Quinn), electroweak baryogensis and several Grand Unified Theories (GUTs). A representative diagram showing the physics process and the branching ratio as a function of tanβ is shown in figure 1. This pseudoscalar Higgs search for "resolved" a particles in the range of 20 to 60 GeV is a good search for new physics. In 2016 this general search was carried out with 35.9 fb^{-1} of data and new competitive limits were set in [7]. Given the improvement in the limits for different 2HDM+S types, this search has garnered attention for the full Run II dataset of CMS.

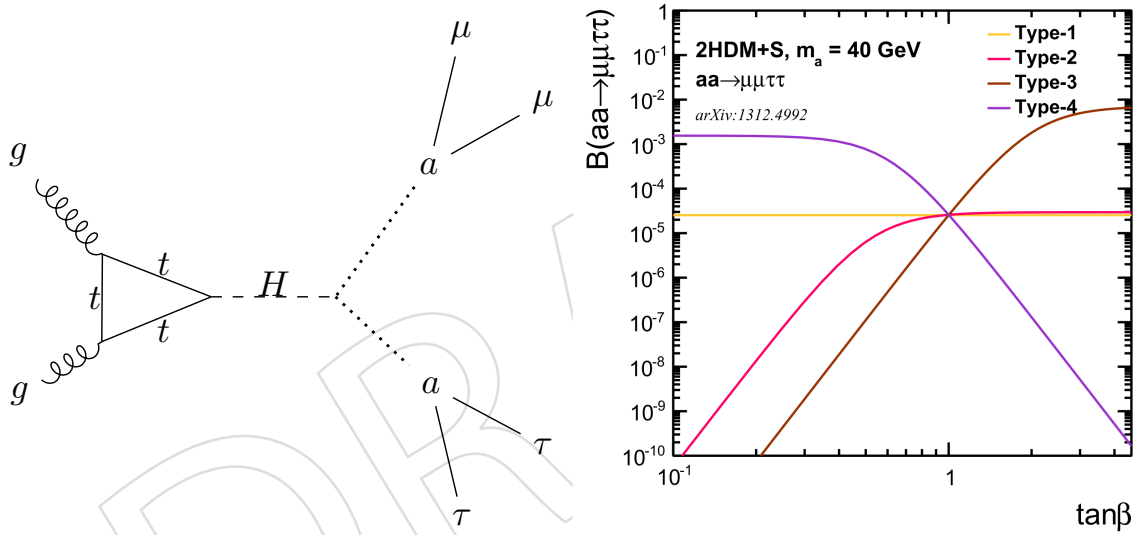

Figure 1: Diagram of Higgs decay to pseudoscalar a particles (Left) and branching ratios for pseudoscalar production in different tanβ scenarios and different 2HDM+S Types (right)

Certain scenarios are entertained using yields provided by different 2HDM+S models. The branching ratios change based on the function of tanβ depending on the type of model under investigation. In particular, we look at types 1-4 which are detailed here [8]. Type III is expected to be most sensitive as it maintains a larger branching ratio compared to other decay modes over the range of the pseudoscalar masses discussed here.

Using the full Run II dataset, more constraints on these models are expected.

2 The CMS detector

From the central interaction point, the CMS detector hosts a silicon pixel and strip tracker, a lead tungstate crystal electromagnetic calorimeter (ECAL), and a brass and scintillator hadron calorimeter (HCAL), each composed of a barrel and two endcap sections. The central feature of

the CMS apparatus is a superconducting solenoid of 6 m internal diameter, providing a magnetic field of 3.8 T. The silicon pixel and tracking systems as well as the calorimeters are contained within the solenoid volume. Muons are detected in gas-ionization chambers embedded in the steel flux-return yoke outside the solenoid.

The nominal pp bunch crossing rate at the LHC is 40 MHz. In order to reduce the rate of events that are recorded for offline analysis, events of interest are selected using a two-tiered trigger system [9]. The first level (L1) is composed of custom built electronics which makes use of high speed optical links and large Field Programmable Gate Arrays (FPGAs). L1 reduces the event rate from the nominal bunch crossing to a rate of around 100 kHz within a time interval of less than 3.5 μs. The second level, known as the High Level Trigger (HLT), consists of a farm of generic processors running a version of the full event reconstruction software that has been optimized for fast processing. The HLT reduces the event rate to about 1 kHz before data storage.

Since the 2012 data taking, significant upgrades of the L1 trigger have benefited this analysis, especially in the final state with two semi-hadronically decaying τ leptons, denoted as τ_{h}. These upgrades improved the τ_{h} identification at L1 by giving more flexibility to object isolation, allowing new techniques to suppress the contribution from additional pp interactions per bunch crossing, and to reconstruct the L1 τ_{h} object in a fiducial region that matches more closely that of a true τ_{h} decay.

A more detailed description of the CMS detector, together with a definition of the coordinate system used and the relevant kinematic variables, can be found in Ref. [10].

3 Simulated samples

The simulation typically used to compare with data is MadGraph5@NLO with PYTHIA 8 for hadronization [11]. These CMS centrally-generated samples are then digitized using GEANT4 [12] to the same format as real data events collected and processed at HLT. This raw data is then reconstructed to physics objects—such as tracks and higher level objects like leptons. A direct comparison between data and simulation can be made after calibrating simulation in control regions.

Data taken from CMS during the entire Run II period was examined, corresponding to 137 fb^{-1} of integrated luminosity. An exhaustive list of data and simulation Monte Carlo (MC) can be found in appendix 10.

3.1 Standard Model Processes

3.2 2 μ 2 τ Signal Samples

For the Monte Carlo production of the signal samples, to reflect the 2HDM modeling, events were generated at tree level for a pseudoscalar Higgs like boson between the masses of 15 and 60 in intervals of 5 GeV with gluon fusion production. These masses are sufficient for the parametric modeling described in the fit to obtain a more precise peak resolution. MadGraph5@NLO v2.6.5 was used to generate these events with a PYTHIA 8 hadronizer. Privately produced samples were used for 2017 and 2018. However, the scripts and conditions used are located here: `https://github.com/samhiggie/iDM-analysis-AODproducer/tree/haa` . The NMSSMHET model was used to simulate the events. Parameters and information can be seen in the package: https://cms-project-generators.web.cern.ch/cms-project-generators/ .

4 Object Selection

- leading muons must have opposite charge coming from the a
- tau decay products must have opposite charge coming from the other a
- no b-quark identified jets
- signal extraction cuts (not shown in data MC control plots, but used in statistical test)
  - invariant mass of the 4 lepton system cuts based on signal to background ratio and overall event yeild
    - $\mu\mu\mu\tau$ all years at $M_{4l} < 120GeV$
    - $\mu\mu e\tau$ all years at $M_{4l} < 120GeV$
    - $\mu\mu e\mu$ all years at $M_{4l} < 110GeV$
    - $\mu\mu\tau\tau$ 2017 and 2018 at $M_{4l} < 130GeV$ and 2016 at $M_{4l} < 135GeV$
  - $M_{\mu\mu} > M_{\tau\tau}$ (to account for energy loss from neutrinos).

Table 1: additional final state selection cuts

finalstate	cuts
$\mu\mu e\mu$	Iso. μ from $\tau <= 0.2$, Iso. e from $\tau <= 0.15$
$\mu\mu e\tau$	τ_h DNN against μ and e
$\mu\mu\mu\tau$	τ_h DNN against μ and e,Iso. μ from $\tau <= 0.15$
$\mu\mu\tau\tau$	τ_h DNN against μ and e

5 Event selection

5.1 Triggers for event selection

The trigger requirements are inclusive, selecting events that pass single, double, and triple muon triggers. Events that are triggered by the single muon trigger criteria contain muons that are isolated with either 22, 24, and 27 GeV energies. Double muon triggers have a 17 GeV threshold for the leading muon and 8 GeV for the subleading muon. Triple muon triggers are used for the channels that have three muons in the final state and have a descending threshold of 12, 10, and 5 GeV respectively. In addition, to properly select objects that coincide with the trigger, triggers are matched to their corresponding objects. The lepton is matched to the seed and filter bit that is generated at the L1 system. Trigger filter bit matching ensures that the objects and events are correctly triggered.

5.2 Optimizing lepton pair selection

A simple selection algorithm was used to identify good lepton pairs that come from the pseudoscalar a. Standard working point cuts are made, and two oppositely charged, isolated muons with the largest scalar summed p_T are chosen to form the first decay products of the a. Two opposite charged τ leptons with the largest scalar summed p_T are chosen for the second a. This approach increased the signal acceptance compared to choosing mass window cuts to form the a pairs. The pair matching efficiency study done with the preliminary dataset from 2016 is listed in table 2. The dip in efficiency may be explained by the boosted or resolved a particles depending on their mass and decay products. If the a mass is low then it is more relativistic, resulting in collimated leptons. If the a has a higher mass, then it is produced closer to rest and the leptons are identified at a large angle of separation. It is likely that the particle flow

Table 2: Lepton pair matching efficiency

a - Mass	15	20	25	30	35	40	45	50	55	60
Efficiency	0.87	0.82	0.79	0.79	0.79	0.80	0.80	0.83	0.85	0.87

algorithm has a more difficult time in identifying decay products of the a particles in between the mass extremes.

5.3 Optimizing final state event selection

After picking the leading prompt muons from the a decay, the next step is to identify the other a decay by using various leptons in the final state. The final state comprises four leptons: two muons coming from the leading a and two tau leptons coming from the subleading a. These τ leptons can decay leptonically or hadronically, and this analysis counts events from both types of decay. Therefore, event selection is driven to find two prompt muons and all decay products of the tau leptons. Four final states are used: $\mu\mu e\mu$, $\mu\mu e\tau$, $\mu\mu\mu\tau$, and $\mu\mu\tau\tau$. The states $\mu\mu\mu\mu$ or $\mu\mu ee$ are not included, as the expected number of events would be extremely low based on the double leptonic tau decay. For notation, when the final state is listed with a tau, such as $\mu\mu\mu\tau$, the τ is presumed to decay hadronically. The third muon in this context would be coming from a leptonically decaying τ. Additionally, due to convention in plotting, the μ(s) are often marked as m(s) and τ(s) as t(s) like in plot 3. In addition to the kinematic requirements listed in 4, several cuts are made to select final state events. The following list contains cuts common to all channels:

- leading muons must have opposite charge coming from the a
- tau decay products must have opposite charge coming from the other a
- no b-quark identified jets
- signal extraction cuts (not shown in data MC control plots, but used in statistical test)
    - invariant mass of the 4 lepton system cuts based on signal to background ratio and overall event yeild
        - $\mu\mu\mu\tau$ all years at $M_{4l} < 120GeV$
        - $\mu\mu e\tau$ all years at $M_{4l} < 120GeV$
        - $\mu\mu e\mu$ all years at $M_{4l} < 110GeV$
        - $\mu\mu\tau\tau$ 2017 and 2018 at $M_{4l} < 130GeV$ and 2016 at $M_{4l} < 135GeV$
    - $M_{\mu\mu} > M_{\tau\tau}$ (to account for energy loss from neutrinos).

Table 3: additional final state selection cuts

finalstate	cuts
$\mu\mu e\mu$	Iso. μ from $\tau <= 0.2$, Iso. e from $\tau <= 0.15$
$\mu\mu e\tau$	τ_h DNN against μ and e
$\mu\mu\mu\tau$	τ_h DNN against μ and e,Iso. μ from $\tau <= 0.15$
$\mu\mu\tau\tau$	τ_h DNN against μ and e

6 Background estimation

The hadronic τ decays produce jets; therefore, jets coming from other processeses effectively fake the hadronic τ signature. This is a non-trival fake rate that needs to be measured and

accounted for in this analysis. In order to conduct the data driven method, a proportion is made to extract the jet faking tau background using an "ABCD" method.

6.1 Brief outline of the fake rate method

The fake rate function in the same sign (SS) region is *known*. Events passing loose identification—that includes tight indentification—in the opposite sign (OS) region is *known*. Events passing in the tight signal region is *unknown*. Assuming that the loose and tight identification is not dependent on the sign of the leptons. Then one can make the equivalence statement:

$$\frac{\text{Events}_{\text{SS Tight}}}{\text{Events}_{\text{SS Loose}}} \doteq \frac{\text{Events}_{\text{OS Tight}}}{\text{Events}_{\text{OS Loose}}}. \tag{1}$$

To make the expression more precise, the fake rate function is typically parametrized in lepton candidate transverse momentum. Also, prompt MC is subtracted from data, which is motivated by estimating the true jet faking tau background (non-prompt taus). If tau leptons in MC are identified as prompt then it is unlikely that the tau is a jet, so they are removed:

$$f(p_T) = \frac{\text{Data Events}_{\text{S.S. Tight}} - \text{Prompt MC Background}_{\text{S.S. Tight}}}{\text{Data Events}_{\text{S.S. Loose}} - \text{Prompt MC Background}_{\text{S.S. Loose}}}. \tag{2}$$

After the measurement is made for each tau candidate, the fake rate is applied as an event weight—$w(f(p_T))$ a transfer function explained 4—to the opposite sign loose region in order to extrapolate to the tight signal region. So isolating the events in the tight signal region and flipping the relation in equation 1, one obtains the result:

$$\text{Events}_{\text{OS Tight}} = w(f(p_T)) \cdot \text{Events}_{\text{OS Loose}}\,. \tag{3}$$

6.2 Measurement of the fake rate

To measure the fake rate, multiple categories are considered and motivated through the processes which produce jets. As outlined in the SM Higgs decays to tau leptons analysis and its supporting document on fake rate measurements, several regions are used to determine the fake rate [13]. The probability for jets to be misidentified as τ_h candidates is measured using $Z \to \mu\mu$+jets events. The events are selected by requiring 2 OS muons passing the medium muon ID and with with relative isolation less than 0.15, $p_T > 10\,\text{GeV}$, and $|\eta| < 2.4$. The leading muon must have $p_T > 23\,\text{GeV}$ (25 GeV) in 2016 (2017 and 2018) and the event must fire the single muon triggers. The muons are required to be separated by $\Delta R > 0.3$ from each other. On top of the two muons, a τ_h candidate passing the VVVLoose WP of the deep ID against jets is selected. The τ_h candidate must have $p_T > 20\,\text{GeV}$, $|\eta| < 2.3$, and pass the new decay mode finding reconstruction with a veto on 2-prong τ_h. The fake rates are observed to depend with the working points of the deep NN discriminator against electrons, and they are measured separately for several combinations of working points. There is no strong dependence with the working point of the deep NN discriminator against muons. Almost all τ_h candidates selected this way are actually quark- or gluon-jets.

The fake rates are measured as a function of the p_T of the τ_h, separately for different τ_h decay modes (1 prong, 1 prong + π^0, 3 prongs, 3 prongs + π^0). They are taken as the ratio between τ_h candidates selected as described above and passing a tighter isolation WP (as used in the analysis, depending on the final state), and τ_h candidates selected as above without any additional condition. To remove the contribution from real τ_h in the fake rate measurement, events with

genuine τ_h are estimated from simulation, and subtracted from the data before taking the ratio of tightly isolated τ_h to loosely isolated τ_h. These processes with genuine τ_h are essentially WZ and ZZ production with leptonic decays.

The probability for jets to be misidentified as electrons is measured in $\mu\mu$+jets events. The events are selected by requiring 2 OS muons passing the medium muon ID and with with relative isolation less than 0.15, $p_T > 10\,\text{GeV}$, and $|\eta| < 2.4$. The leading muon must have $p_T > 23\,\text{GeV}$ (25 GeV) in 2016 (2017 and 2018) and the event must fire the single muon triggers. The muons are required to be separated by $\Delta R > 0.3$ from each other. On top of the two muons, an electron without ID (other than Gsf electron) nor isolation requirement is selected. It must have $p_T > 10\,\text{GeV}$, $|\eta| < 2.5$, and be separated by $\Delta R > 0.3$ from the muons.

The fake rate is measured as a function of the electron p_T, as the ratio of events selected as above with the additional requirement that the electron must pass the WP90 ID and the relative isolation less than 0.15, to events selected as above. In the numerator, the fraction of events selected in data with a genuine electron is significant. We estimate it from simulation and control its normalization is predicted correctly by looking at the distribution of the transverse mass between the electron and the p_T^{miss}, as shown in Fig **??** for the different data taking periods. We veto all events with $m_T > 40\,\text{GeV}$ to measure the electron fake rate to get a purer event selection, and we subtract the remaining genuine electron backgrounds based on simulation estimations.

The probability for jets to be misidentified as muons is measured in ee+jets events. The events are selected by requiring 2 OS electrons passing the MVA electron ID WP90 and with with relative isolation less than 0.15, $p_T > 10\,\text{GeV}$, and $|\eta| < 2.5$. The leading electron must have $p_T > 26\,\text{GeV}$ in 2016, $p_T > 28\,\text{GeV}$ in 2017, and $p_T > 33\,\text{GeV}$ in 2018, and the event must fire the single electron triggers. The electrons are required to be separated by $\Delta R > 0.3$ from each other. On top of the two electrons, an muon without ID (other than global or tracker muon) nor isolation requirement is selected. It must have $p_T > 10\,\text{GeV}$, $|\eta| < 2.5$, and be separated by $\Delta R > 0.3$ from the electrons.

The fake rate is measured as a function of the muon p_T, as the ratio of events selected as above with the additional requirement that the muon must pass the medium ID and the relative isolation less than 0.15, to events selected as above. In the numerator, the fraction of events selected in data with a genuine muon is significant. We estimate it from simulation and control its normalization is predicted correctly by looking at the distribution of the transverse mass between the muon and the p_T^{miss}, as shown in Fig **??** for the different data taking periods. We veto all events with $m_T > 40\,\text{GeV}$ to measure the muon fake rate to get a purer event selection, and we subtract the remaining genuine muon backgrounds based on simulation estimations.

6.3 Application of the fake rate method

After the jet faking tau rate is measured, it is then applied to events that are identified as loose and not tight. Since the final state involves two tau leptons, this procedure is applied to each tau lepton in the final state, thus requiring application of the fake rate in three different scenarios. The final weight is then applied depending on the pass and fail criteria of each lepton candidate. In the scenario where the event fails both candidate requirements, then a minus sign is included, to avoid the case of double counting. The weight is effectively a transfer factor that is created using the fake rate measured earlier. The transfer factor has its form because the weight is the ratio of tight to loose—tight excluded—instead of tight to loose—tight included.

- If event fails identification for τ 1:

$$w_1(p_T) = \frac{f_1(p_T)}{1 - f_1(p_T)} \tag{4}$$

- If event fails identification for τ 2:

$$w_2(p_T) = \frac{f_2(p_T)}{1 - f_2(p_T)} \tag{5}$$

- If event fails identification for both:

$$w_{12}(p_T) = -\frac{f_1(p_T)}{1 - f_1(p_T)} \cdot \frac{f_2(p_T)}{1 - f_2(p_T)} \tag{6}$$

To illustrate the different regions in the ABCD method along with each tau candidate, a diagram was drawn depicting the scenarios and is shown in figure **??**.

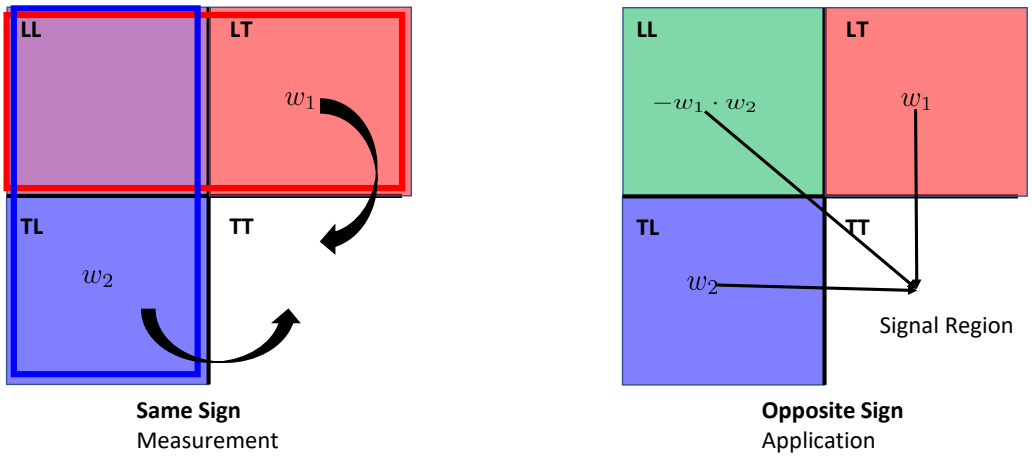

Figure 2: ABCD method diagram depicting the measurement and application regions for each τ_h lepton in the final sate.

This fake factor methodology has been used by other analyses such as the SM Higgs measurement with an associated Z boson [14].

For a closure test, the same criteria are applied to the selection of the tight same sign region. The vast majority of the background should be jets faking taus in that case. Indeed it is shown in figure 3 on the right.

7 Statistical Inference Modeling and Uncertainties

In order to measure the systematic effects on the final fit distributions, changes in the fit templates are done and propagated to the fit model in the form of rate parameters. These rate parameters differ slightly between the signal and background distributions. For background, the error in the fit parameters is directly included in the uncertainty model.

The uncertainty of the spline function affects the uncertainty for the signal, so it is included in the fit model. As mentioned in the fit model section **??** and shown in figure **??**, the magnitude

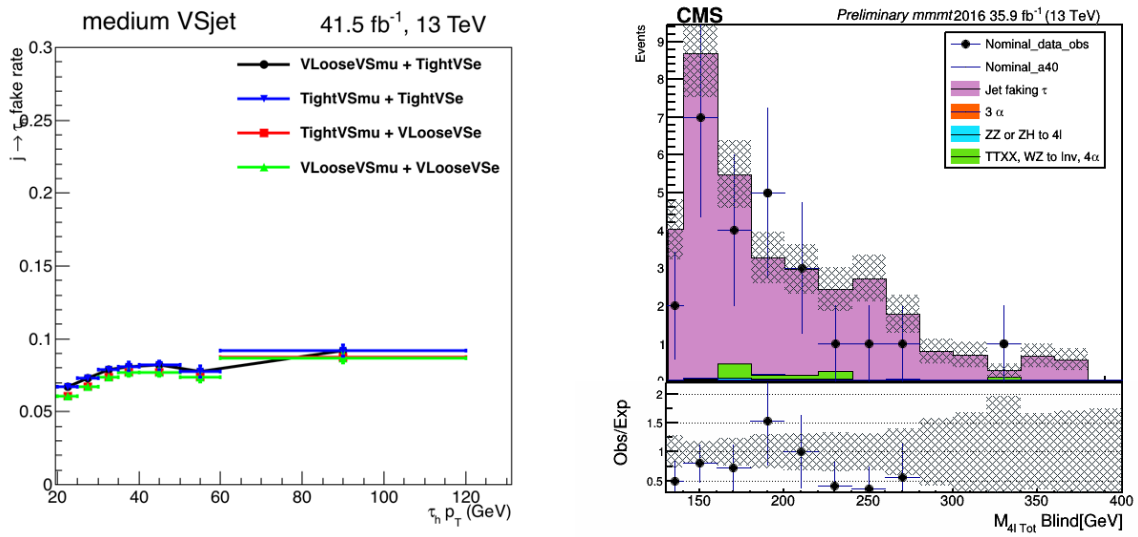

Figure 3: (Left)Fake rates for jets misidentified as τ_h for the Medium deep ID WP against jets, in 1 prong + π^0 with 2017 data. (Right) Validation of the fake factor method. Fake factors are applied to the same sign tight region.

of this uncertainty is estimated from the fit of the parameters for the spline. Overall, a 10% uncertainty is used for the Lorentzian (alpha) and 20% for the standard deviation (sigma) and 0.5% for the mean (mean). Although the mean is measured very precisely, the energy scale shifts from the leptons are included in this number. The shift should fit within the envelope of the percentage on the parameter for it to be modeled correctly.

For the other systematic uncertainties that are not based on parametric shapes, like the energy scale of the leptons, a log-normal deviation to the normalization is used.

8 Results

After the final event selection, including the signal extraction cuts listed in section 5.2, the statistical hypothesis test can be made. The final number of events listed in each category for the full Run II dataset is shown in the table **??** below.

Year	Signal Total	Background Total		
	$m_a = 40$ GeV	Data Driven (FF)	Irreducible (ZZ)	Total
2016	16.15	3.21	1.43	4.64
2017	19.49	6.63	3.26	9.89
2018	27.45	14.93	2.79	17.72
Run II	63.09	24.77	7.48	32.25

Table 4: Expected event yields of signal and background categories across all years with 137 fb^{-1} of data. Signal normalized to .01% of the SM Higgs Branching Fraction.

.

As discussed in the previous section **??**, the shapes that were created are used in an upper limit for each mass point. Initial values of the signal distributions are selected to make sure that the signal strength modifier (μ) in the limit is of order unity. The range of masses in the limit is between 20 GeV and 60 GeV to ensure compatibility with $h \to aa$ combination limits for additional exotic Higgs models—like those at lower a mass. In order to estimate the upper limit

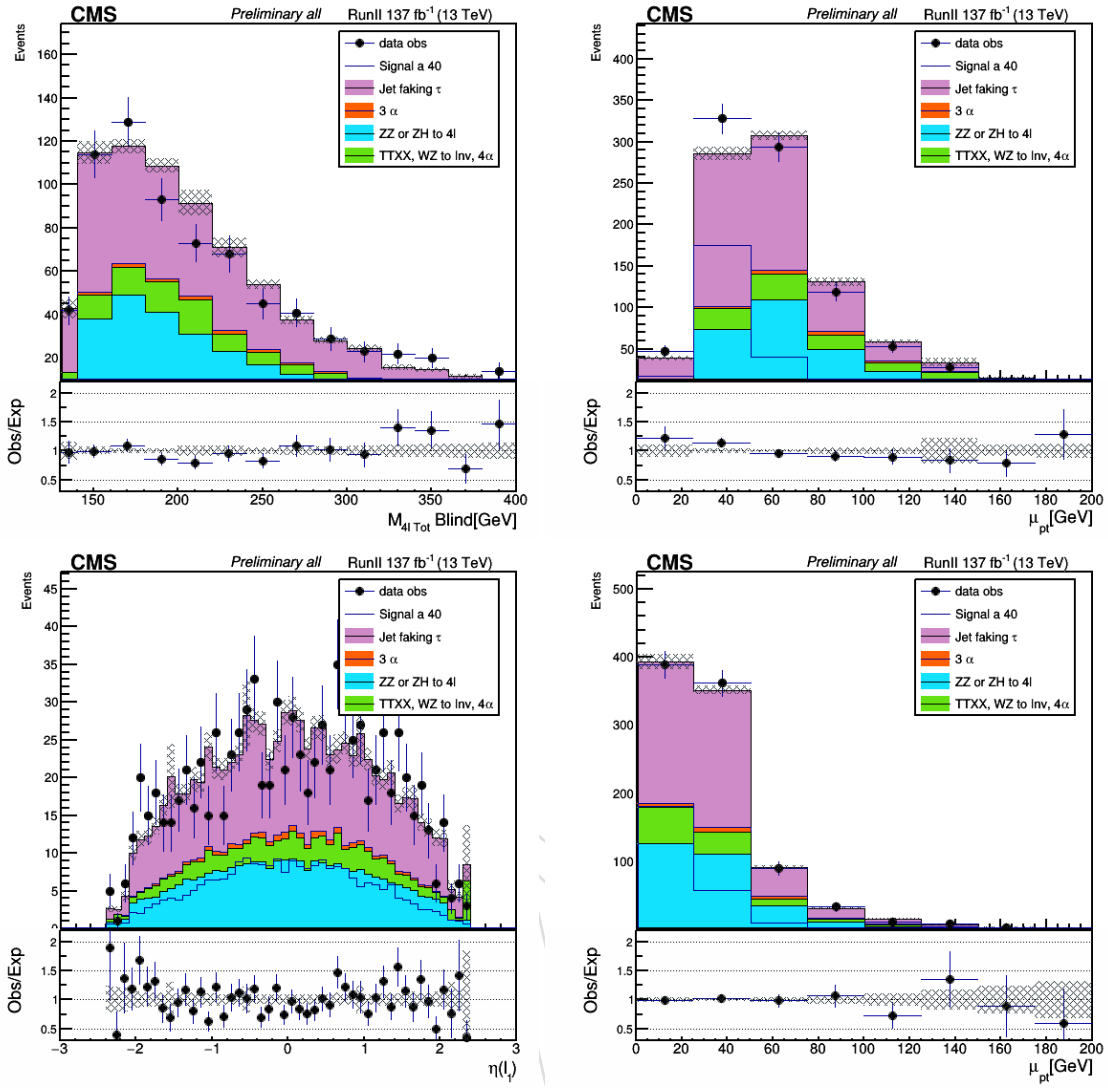

Figure 4: Several data MC control plots for the combination of the full Run II dataset and all final states.

at 95% CL on the branching fraction, a simple Poisson model can be used. For a statistically limited search, we can estimate the background yield as no events. The estimated upper limit on the branching fraction calculated earlier is:

$$B = \frac{N}{\sigma \cdot A \cdot \mathcal{L}} = 0.00043. \tag{7}$$

This limit is set by adjusting the signal strength (event yield) until a p-value of 5% is reached on the joint likelihood function for the fit model. The event yield is normalized with a branching fraction, which was assumed to be $\sigma_{SM}(h) \times 0.01\%$. Multiplying the CL by 0.01% returns the limit on $\frac{\sigma_h}{\sigma_{SM}} B(h \rightarrow aa \rightarrow 2\mu 2\tau)$. Preliminary limits are set using the asymptotic limit method [15] for each mass point.

All of the years and channels are then added together to form the combined result **??** and the model 2HDM+S interpretations for different scenarios. Type III, where coupling to τ leptons is favored, is expected to be the most stringent scenario for this analysis. More parameter space in theory is excluded at the upper 95% level in regions of lower values on the limit (regions in blue) in figure 6. Type I excludes mostly high mass particles and isn't depended on tan β. Type II and III exclude more at the high tan β region as opposed to Type IV which excludes at the low tan β region.

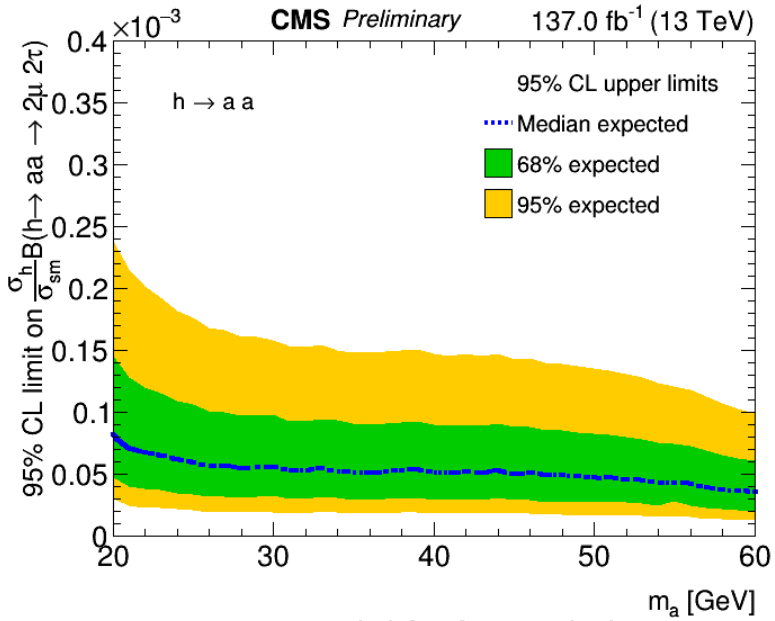

Figure 5: Asymptotic upper 95% CL Limits on the branching fraction times ratio of the SM cross section for the full Run II dataset (137fb^{-1})

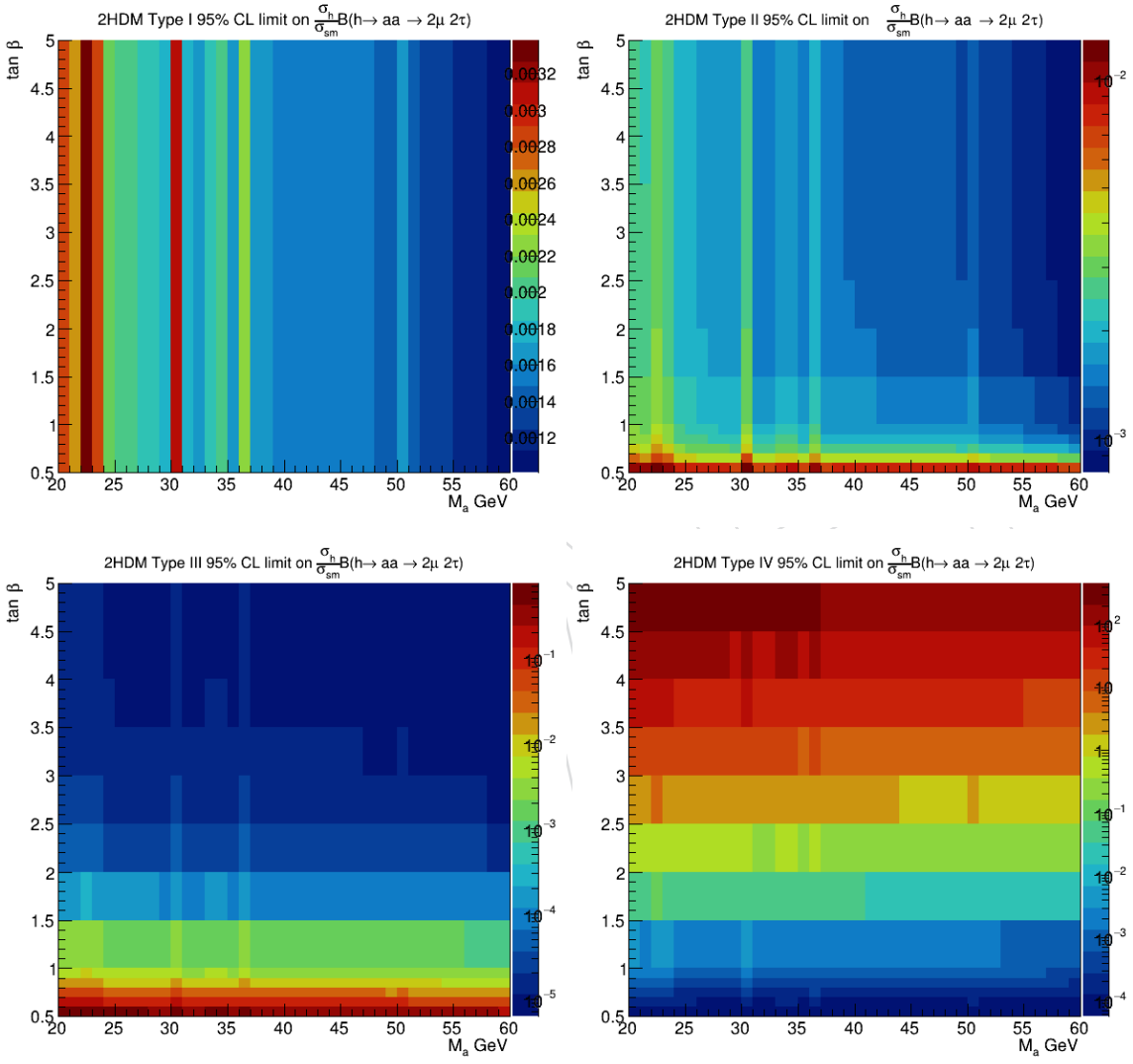

Figure 6: upper 95% CL limits on the branch fraction of $h \to aa$ times the ratio of the SM cross sections for the full Run II dataset (137fb^{-1}) for different 2HDM+S model specific scenarios plotted also as a function of tan β.

9 Summary

Using the full Run II dataset collected at CMS corresponding to an integrated luminosity of 137fb^{-1}, the search for the SM Higgs Boson, h, decaying to a pair of pseudoscalars, a, which then decay to pairs of muons and tau leptons was completed. Expected upper 95% confidence level limits are set to about 10^{-4} after the addition of all final final states. These results are independent of separate 2HDM+S models and is considered a generic search that applies to multiple MSSM scenarios along with any BSM physics within the search window.

10 Appendix

The full Run II dataset was used corresponding to 137fb^{-1}. The golden JSON files were used for correct intervals of validity (IOVs) for each year 5.

Table 5: Certified JSON files for RunII IOVs

Cert_271036-284044_13TeV_ReReco_07Aug2017_Collisions16_JSON.txt
Cert_294927-306462_13TeV_EOY2017ReReco_Collisions17_JSON.txt
Cert_314472-325175_13TeV_17SeptEarlyReReco2018ABC_PromptEraD_Collisions18_JSON.txt

Data for 2016

Table 6: List of data sets included in the analysis for the 2016 data taking period.

Data set
/SingleMuon/Run2016B_ver2-Nano25Oct2019_ver2-v1/NANOAOD
/SingleMuon/Run2016B_ver1-Nano25Oct2019_ver1-v1/NANOAOD
/SingleMuon/Run2016G-Nano25Oct2019-v1/NANOAOD
/SingleMuon/Run2016F-Nano25Oct2019-v1/NANOAOD
/SingleMuon/Run2016E-Nano25Oct2019-v1/NANOAOD
/SingleMuon/Run2016D-Nano25Oct2019-v1/NANOAOD
/SingleMuon/Run2016C-Nano25Oct2019-v1/NANOAOD
/SingleMuon/Run2016H-Nano25Oct2019-v1/NANOAOD
/DoubleMuon/Run2016H-Nano25Oct2019-v1/NANOAOD
/DoubleMuon/Run2016G-Nano25Oct2019-v1/NANOAOD
/DoubleMuon/Run2016F-Nano25Oct2019-v1/NANOAOD
/DoubleMuon/Run2016B_ver2-Nano25Oct2019_ver2-v1/NANOAOD
/DoubleMuon/Run2016B_ver1-Nano25Oct2019_ver1-v1/NANOAOD
/DoubleMuon/Run2016E-Nano25Oct2019-v1/NANOAOD
/DoubleMuon/Run2016D-Nano25Oct2019-v1/NANOAOD
/DoubleMuon/Run2016C-Nano25Oct2019-v1/NANOAOD

Data for 2017

Data for 2018

Table 7: List of data sets included in the analysis for the 2017 data taking period.

Data set
/DoubleMuon/Run2017B-02Apr2020-v1/NANOAOD
/DoubleMuon/Run2017C-02Apr2020-v1/NANOAOD
/DoubleMuon/Run2017D-02Apr2020-v1/NANOAOD
/DoubleMuon/Run2017E-02Apr2020-v1/NANOAOD
/DoubleMuon/Run2017F-02Apr2020-v1/NANOAOD
/MuonEG/Run2017B-02Apr2020-v1/NANOAOD
/MuonEG/Run2017C-02Apr2020-v1/NANOAOD
/MuonEG/Run2017D-02Apr2020-v1/NANOAOD
/MuonEG/Run2017E-02Apr2020-v1/NANOAOD
/MuonEG/Run2017F-02Apr2020-v1/NANOAOD
/SingleMuon/Run2017B-02Apr2020-v1/NANOAOD
/SingleMuon/Run2017C-02Apr2020-v1/NANOAOD
/SingleMuon/Run2017D-02Apr2020-v1/NANOAOD
/SingleMuon/Run2017E-02Apr2020-v1/NANOAOD
/SingleMuon/Run2017F-02Apr2020-v1/NANOAOD
/DoubleEG/Run2017B-02Apr2020-v1/NANOAOD
/DoubleEG/Run2017C-02Apr2020-v1/NANOAOD
/DoubleEG/Run2017D-02Apr2020-v1/NANOAOD
/DoubleEG/Run2017E-02Apr2020-v1/NANOAOD
/DoubleEG/Run2017F-02Apr2020-v1/NANOAOD
/SingleElectron/Run2017B-02Apr2020-v1/NANOAOD
/SingleElectron/Run2017C-02Apr2020-v1/NANOAOD
/SingleElectron/Run2017D-02Apr2020-v1/NANOAOD
/SingleElectron/Run2017E-02Apr2020-v1/NANOAOD
/SingleElectron/Run2017F-02Apr2020-v1/NANOAOD

Table 8: List of data sets included in the analysis for the 2018 data taking period.

Data set
/SingleMuon/Run2018A-02Apr2020-v1/NANOAOD
/SingleMuon/Run2018B-02Apr2020-v1/NANOAOD
/SingleMuon/Run2018C-02Apr2020-v1/NANOAOD
/SingleMuon/Run2018D-02Apr2020-v1/NANOAOD
/DoubleMuon/Run2018A-02Apr2020-v1/NANOAOD
/DoubleMuon/Run2018B-02Apr2020-v1/NANOAOD
/DoubleMuon/Run2018C-02Apr2020-v1/NANOAOD
/DoubleMuon/Run2018D-02Apr2020-v1/NANOAOD
/DoubleMuonLowMass/Run2018A-02Apr2020-v1/NANOAOD
/DoubleMuonLowMass/Run2018B-02Apr2020-v1/NANOAOD
/DoubleMuonLowMass/Run2018C-02Apr2020-v1/NANOAOD
/DoubleMuonLowMass/Run2018D-02Apr2020-v1/NANOAOD
/EGamma/Run2018A-02Apr2020-v1/NANOAOD
/EGamma/Run2018B-02Apr2020-v1/NANOAOD
/EGamma/Run2018C-02Apr2020-v1/NANOAOD
/EGamma/Run2018D-02Apr2020-v1/NANOAOD

Table 9: List of data sets included in the analysis for the 2016 data taking period.

Monte Carlo Datasets for 2016
/W1JetsToLNu_TuneCUETP8M1_13TeV-madgraphMLM-pythia8/RunIISummer16NanoAODv7-PUMoriond17_Nano02Apr2020_102X_mcRun2_asymptotic_v8-v1/NANOAODSIM
/W2JetsToLNu_TuneCUETP8M1_13TeV-madgraphMLM-pythia8/RunIISummer16NanoAODv7-PUMoriond17_Nano02Apr2020_102X_mcRun2_asymptotic_v8_ext1-v1/NANOAODSIM
/W2JetsToLNu_TuneCUETP8M1_13TeV-madgraphMLM-pythia8/RunIISummer16NanoAODv7-PUMoriond17_Nano02Apr2020_102X_mcRun2_asymptotic_v8-v1/NANOAODSIM
/W3JetsToLNu_TuneCUETP8M1_13TeV-madgraphMLM-pythia8/RunIISummer16NanoAODv7-PUMoriond17_Nano02Apr2020_102X_mcRun2_asymptotic_v8_ext1-v1/NANOAODSIM
/W3JetsToLNu_TuneCUETP8M1_13TeV-madgraphMLM-pythia8/RunIISummer16NanoAODv7-PUMoriond17_Nano02Apr2020_102X_mcRun2_asymptotic_v8-v1/NANOAODSIM
/W4JetsToLNu_TuneCUETP8M1_13TeV-madgraphMLM-pythia8/RunIISummer16NanoAODv7-PUMoriond17_Nano02Apr2020_102X_mcRun2_asymptotic_v8_ext1-v1/NANOAODSIM
/W4JetsToLNu_TuneCUETP8M1_13TeV-madgraphMLM-pythia8/RunIISummer16NanoAODv7-PUMoriond17_Nano02Apr2020_102X_mcRun2_asymptotic_v8_ext2-v1/NANOAODSIM
/W4JetsToLNu_TuneCUETP8M1_13TeV-madgraphMLM-pythia8/RunIISummer16NanoAODv7-PUMoriond17_Nano02Apr2020_102X_mcRun2_asymptotic_v8-v1/NANOAODSIM
/WJetsToLNu_TuneCUETP8M1_13TeV-madgraphMLM-pythia8/RunIISummer16NanoAODv7-PUMoriond17_Nano02Apr2020_102X_mcRun2_asymptotic_v8_ext2-v1/NANOAODSIM
/WJetsToLNu_TuneCUETP8M1_13TeV-madgraphMLM-pythia8/RunIISummer16NanoAODv7-PUMoriond17_Nano02Apr2020_102X_mcRun2_asymptotic_v8-v1/NANOAODSIM
/DY1JetsToLL_M-50_TuneCUETP8M1_13TeV-madgraphMLM-pythia8/RunIISummer16NanoAODv7-PUMoriond17_Nano02Apr2020_102X_mcRun2_asymptotic_v8-v1/NANOAODSIM
/DY2JetsToLL_M-50_TuneCUETP8M1_13TeV-madgraphMLM-pythia8/RunIISummer16NanoAODv7-PUMoriond17_Nano02Apr2020_102X_mcRun2_asymptotic_v8-v1/NANOAODSIM
/DY3JetsToLL_M-50_TuneCUETP8M1_13TeV-madgraphMLM-pythia8/RunIISummer16NanoAODv7-PUMoriond17_Nano02Apr2020_102X_mcRun2_asymptotic_v8-v1/NANOAODSIM
/DY4JetsToLL_M-50_TuneCUETP8M1_13TeV-madgraphMLM-pythia8/RunIISummer16NanoAODv7-PUMoriond17_Nano02Apr2020_102X_mcRun2_asymptotic_v8-v1/NANOAODSIM
/DYJetsToLL_M-50_TuneCUETP8M1_13TeV-madgraphMLM-pythia8/RunIISummer16NanoAODv7-PUMoriond17_Nano02Apr2020_102X_mcRun2_asymptotic_v8_ext1-v1/NANOAODSIM
/DYJetsToLL_M-50_TuneCUETP8M1_13TeV-madgraphMLM-pythia8/RunIISummer16NanoAODv7-PUMoriond17_Nano02Apr2020_102X_mcRun2_asymptotic_v8_ext2-v1/NANOAODSIM
/DYJetsToLL_M-10to50_TuneCUETP8M1_13TeV-madgraphMLM-pythia8/RunIISummer16NanoAODv7-PUMoriond17_Nano02Apr2020_102X_mcRun2_asymptotic_v8-v1/NANOAODSIM
/WZTo3LNu_TuneCUETP8M1_13TeV-powheg-pythia8/RunIISummer16NanoAODv7-PUMoriond17_Nano02Apr2020_102X_mcRun2_asymptotic_v8-v1/NANOAODSIM
/WWW_4F_TuneCUETP8M1_13TeV-amcatnlo-pythia8/RunIISummer16NanoAODv7-PUMoriond17_Nano02Apr2020_102X_mcRun2_asymptotic_v8-v1/NANOAODSIM
/WWZ_TuneCUETP8M1_13TeV-amcatnlo-pythia8/RunIISummer16NanoAODv7-PUMoriond17_Nano02Apr2020_102X_mcRun2_asymptotic_v8-v1/NANOAODSIM
/WZZ_TuneCUETP8M1_13TeV-amcatnlo-pythia8/RunIISummer16NanoAODv7-PUMoriond17_Nano02Apr2020_102X_mcRun2_asymptotic_v8-v1/NANOAODSIM
/ZZZ_TuneCUETP8M1_13TeV-amcatnlo-pythia8/RunIISummer16NanoAODv7-PUMoriond17_Nano02Apr2020_102X_mcRun2_asymptotic_v8-v1/NANOAODSIM
/ttZJets_13TeV_madgraphMLM-pythia8/RunIISummer16NanoAODv7-PUMoriond17_Nano02Apr2020_102X_mcRun2_asymptotic_v8-v1/NANOAODSIM
/ttWJets_13TeV_madgraphMLM/RunIISummer16NanoAODv7-Nano02Apr2020_102X_mcRun2_asymptotic_v8-v1/NANOAODSIM
/GluGluToContinToZZTo2e2mu_13TeV_MCFM701_pythia8/RunIISummer16NanoAODv7-PUMoriond17_Nano02Apr2020_102X_mcRun2_asymptotic_v8-v1/NANOAODSIM
/GluGluToContinToZZTo2e2nu_13TeV_MCFM701_pythia8/RunIISummer16NanoAODv7-PUMoriond17_Nano02Apr2020_102X_mcRun2_asymptotic_v8-v1/NANOAODSIM
/GluGluToContinToZZTo2e2tau_13TeV_MCFM701_pythia8/RunIISummer16NanoAODv7-PUMoriond17_Nano02Apr2020_102X_mcRun2_asymptotic_v8-v1/NANOAODSIM
/GluGluToContinToZZTo2mu2nu_13TeV_MCFM701_pythia8/RunIISummer16NanoAODv7-PUMoriond17_Nano02Apr2020_102X_mcRun2_asymptotic_v8-v1/NANOAODSIM
/GluGluToContinToZZTo2mu2tau_13TeV_MCFM701_pythia8/RunIISummer16NanoAODv7-PUMoriond17_Nano02Apr2020_102X_mcRun2_asymptotic_v8-v1/NANOAODSIM
/GluGluToContinToZZTo4e_13TeV_MCFM701_pythia8/RunIISummer16NanoAODv7-PUMoriond17_Nano02Apr2020_102X_mcRun2_asymptotic_v8-v1/NANOAODSIM
/GluGluToContinToZZTo4mu_13TeV_MCFM701_pythia8/RunIISummer16NanoAODv7-PUMoriond17_Nano02Apr2020_102X_mcRun2_asymptotic_v8-v1/NANOAODSIM
/GluGluToContinToZZTo4tau_13TeV_MCFM701_pythia8/RunIISummer16NanoAODv7-PUMoriond17_Nano02Apr2020_102X_mcRun2_asymptotic_v8-v1/NANOAODSIM
/GluGluZH_HToWW_M125_13TeV_powheg_pythia8/RunIISummer16NanoAODv7-PUMoriond17_Nano02Apr2020_102X_mcRun2_asymptotic_v8-v1/NANOAODSIM
/HZJ_HToWW_M125_13TeV_powheg_pythia8/RunIISummer16NanoAODv7-PUMoriond17_Nano02Apr2020_102X_mcRun2_asymptotic_v8-v1/NANOAODSIM
/ZZTo4L_13TeV_powheg_pythia8/RunIISummer16NanoAODv7-PUMoriond17_Nano02Apr2020_102X_mcRun2_asymptotic_v8-v1/NANOAODSIM
/ggZH_HToTauTau_ZToLL_M125_13TeV_powheg_pythia8/RunIISummer16NanoAODv7-PUMoriond17_Nano02Apr2020_102X_mcRun2_asymptotic_v8-v1/NANOAODSIM
/ggZH_HToTauTau_ZToNuNu_M125_13TeV_powheg_pythia8/RunIISummer16NanoAODv7-PUMoriond17_Nano02Apr2020_102X_mcRun2_asymptotic_v8-v1/NANOAODSIM
/ggZH_HToTauTau_ZToQQ_M125_13TeV_powheg_pythia8/RunIISummer16NanoAODv7-PUMoriond17_Nano02Apr2020_102X_mcRun2_asymptotic_v8-v1/NANOAODSIM
/ZHToTauTau_M125_13TeV_powheg_pythia8/RunIISummer16NanoAODv7-PUMoriond17_Nano02Apr2020_102X_mcRun2_asymptotic_v8-v1/NANOAODSIM
/WminusHToTauTau_M125_13TeV_powheg_pythia8/RunIISummer16NanoAODv7-PUMoriond17_Nano02Apr2020_102X_mcRun2_asymptotic_v8-v1/NANOAODSIM
/WplusHToTauTau_M125_13TeV_powheg_pythia8/RunIISummer16NanoAODv7-PUMoriond17_Nano02Apr2020_102X_mcRun2_asymptotic_v8-v1/NANOAODSIM
/HWminusJ_HToWW_M125_13TeV_powheg_pythia8/RunIISummer16NanoAODv7-PUMoriond17_Nano02Apr2020_102X_mcRun2_asymptotic_v8-v1/NANOAODSIM
/HWplusJ_HToWW_M125_13TeV_powheg_pythia8/RunIISummer16NanoAODv7-PUMoriond17_Nano02Apr2020_102X_mcRun2_asymptotic_v8-v1/NANOAODSIM
/SUSYGluGluToHToAA_AToMuMu_AToTauTau_M-15_TuneCUETP8M1_13TeV_madgraph_pythia8/RunIISummer16NanoAODv7-PUMoriond17_Nano02Apr2020_102X_mcRun2_asymptotic_v8-v1/NANOAODSIM
/SUSYGluGluToHToAA_AToMuMu_AToTauTau_M-20_TuneCUETP8M1_13TeV_madgraph_pythia8/RunIISummer16NanoAODv7-PUMoriond17_Nano02Apr2020_102X_mcRun2_asymptotic_v8-v1/NANOAODSIM
/SUSYGluGluToHToAA_AToMuMu_AToTauTau_M-25_TuneCUETP8M1_13TeV_madgraph_pythia8/RunIISummer16NanoAODv7-PUMoriond17_Nano02Apr2020_102X_mcRun2_asymptotic_v8-v1/NANOAODSIM
/SUSYGluGluToHToAA_AToMuMu_AToTauTau_M-30_TuneCUETP8M1_13TeV_madgraph_pythia8/RunIISummer16NanoAODv7-PUMoriond17_Nano02Apr2020_102X_mcRun2_asymptotic_v8-v1/NANOAODSIM
/SUSYGluGluToHToAA_AToMuMu_AToTauTau_M-35_TuneCUETP8M1_13TeV_madgraph_pythia8/RunIISummer16NanoAODv7-PUMoriond17_Nano02Apr2020_102X_mcRun2_asymptotic_v8-v1/NANOAODSIM
/SUSYGluGluToHToAA_AToMuMu_AToTauTau_M-40_TuneCUETP8M1_13TeV_madgraph_pythia8/RunIISummer16NanoAODv7-PUMoriond17_Nano02Apr2020_102X_mcRun2_asymptotic_v8-v1/NANOAODSIM
/SUSYGluGluToHToAA_AToMuMu_AToTauTau_M-45_TuneCUETP8M1_13TeV_madgraph_pythia8/RunIISummer16NanoAODv7-PUMoriond17_Nano02Apr2020_102X_mcRun2_asymptotic_v8-v1/NANOAODSIM
/SUSYGluGluToHToAA_AToMuMu_AToTauTau_M-50_TuneCUETP8M1_13TeV_madgraph_pythia8/RunIISummer16NanoAODv7-PUMoriond17_Nano02Apr2020_102X_mcRun2_asymptotic_v8-v1/NANOAODSIM
/SUSYGluGluToHToAA_AToMuMu_AToTauTau_M-55_TuneCUETP8M1_13TeV_madgraph_pythia8/RunIISummer16NanoAODv7-PUMoriond17_Nano02Apr2020_102X_mcRun2_asymptotic_v8-v1/NANOAODSIM
/SUSYGluGluToHToAA_AToMuMu_AToTauTau_M-60_TuneCUETP8M1_13TeV_madgraph_pythia8/RunIISummer16NanoAODv7-PUMoriond17_Nano02Apr2020_102X_mcRun2_asymptotic_v8-v1/NANOAODSIM

Table 10: List of data sets included in the analysis for the 2017 data taking period.

Monte Carlo Datasets for 2017
/DY1JetsToLL_M-50_TuneCP5_13TeV-madgraphMLM-pythia8/RunIIFall17NanoAODv7-PU2017_12Apr2018_Nano02Apr2020_new_pmx_102X_mc2017_realistic_v8-v1/NANOAODSIM
/DY1JetsToLL_M-50_TuneCP5_13TeV-madgraphMLM-pythia8/RunIIFall17NanoAODv7-PU2017_12Apr2018_Nano02Apr2020_v3_102X_mc2017_realistic_v8_ext1-v1/NANOAODSIM
/DY2JetsToLL_M-50_TuneCP5_13TeV-madgraphMLM-pythia8/RunIIFall17NanoAODv7-PU2017_12Apr2018_Nano02Apr2020_102X_mc2017_realistic_v8-v1/NANOAODSIM
/DY2JetsToLL_M-50_TuneCP5_13TeV-madgraphMLM-pythia8/RunIIFall17NanoAODv7-PU2017_12Apr2018_Nano02Apr2020_102X_mc2017_realistic_v8_ext1-v1/NANOAODSIM
/DY3JetsToLL_M-50_TuneCP5_13TeV-madgraphMLM-pythia8/RunIIFall17NanoAODv7-PU2017_12Apr2018_Nano02Apr2020_102X_mc2017_realistic_v8-v1/NANOAODSIM
/DY3JetsToLL_M-50_TuneCP5_13TeV-madgraphMLM-pythia8/RunIIFall17NanoAODv7-PU2017_12Apr2018_Nano02Apr2020_102X_mc2017_realistic_v8_ext1-v1/NANOAODSIM
/DY4JetsToLL_M-50_TuneCP5_13TeV-madgraphMLM-pythia8/RunIIFall17NanoAODv7-PU2017_12Apr2018_Nano02Apr2020_v2_102X_mc2017_realistic_v8-v1/NANOAODSIM
/DYJetsToLL_M-50_TuneCP5_13TeV-madgraphMLM-pythia8/RunIIFall17NanoAODv7-PU2017RECOSIMstep_12Apr2018_Nano02Apr2020_102X_mc2017_realistic_v8-v1/NANOAODSIM
/DYJetsToLL_M-50_TuneCP5_13TeV-madgraphMLM-pythia8/RunIIFall17NanoAODv7-PU2017RECOSIMstep_12Apr2018_Nano02Apr2020_102X_mc2017_realistic_v8_ext1-v1/NANOAODSIM
/DYJetsToLL_M-10to50_TuneCP5_13TeV-madgraphMLM-pythia8/RunIIFall17NanoAODv7-PU2017_12Apr2018_Nano02Apr2020_102X_mc2017_realistic_v8-v1/NANOAODSIM
/DYJetsToLL_M-10to50_TuneCP5_13TeV-madgraphMLM-pythia8/RunIIFall17NanoAODv7-PU2017_12Apr2018_Nano02Apr2020_102X_mc2017_realistic_v8_ext1-v1/NANOAODSIM
/W1JetsToLNu_TuneCP5_13TeV-madgraphMLM-pythia8/RunIIFall17NanoAODv7-PU2017_12Apr2018_Nano02Apr2020_ext_102X_mc2017_realistic_v8-v1/NANOAODSIM
/W2JetsToLNu_TuneCP5_13TeV-madgraphMLM-pythia8/RunIIFall17NanoAODv7-PU2017_12Apr2018_Nano02Apr2020_EXT_102X_mc2017_realistic_v8-v1/NANOAODSIM
/W3JetsToLNu_TuneCP5_13TeV-madgraphMLM-pythia8/RunIIFall17NanoAODv7-PU2017_12Apr2018_Nano02Apr2020_PU2017_102X_mc2017_realistic_v8-v1/NANOAODSIM
/W4JetsToLNu_TuneCP5_13TeV-madgraphMLM-pythia8/RunIIFall17NanoAODv7-PU2017_12Apr2018_Nano02Apr2020_new_pmx_102X_mc2017_realistic_v8-v1/NANOAODSIM
/WJetsToLNu_TuneCP5_13TeV-madgraphMLM-pythia8/RunIIFall17NanoAODv7-PU2017_12Apr2018_Nano02Apr2020_102X_mc2017_realistic_v8_ext1-v1/NANOAODSIM
/WJetsToLNu_TuneCP5_13TeV-madgraphMLM-pythia8/RunIIFall17NanoAODv7-PU2017_12Apr2018_Nano02Apr2020_EXT_102X_mc2017_realistic_v8-v1/NANOAODSIM
/WZTo3LNu_13TeV-powheg-pythia8/RunIIFall17NanoAODv7-PU2017_12Apr2018_Nano02Apr2020_102X_mc2017_realistic_v8-v1/NANOAODSIM
/WWW_4F_TuneCP5_13TeV-amcatnlo-pythia8/RunIIFall17NanoAODv7-PU2017_12Apr2018_Nano02Apr2020_EXT_102X_mc2017_realistic_v8-v1/NANOAODSIM
/WWZ_4F_TuneCP5_13TeV-amcatnlo-pythia8/RunIIFall17NanoAODv7-PU2017_12Apr2018_Nano02Apr2020_EXT_102X_mc2017_realistic_v8-v1/NANOAODSIM
/WZZ_TuneCP5_13TeV-amcatnlo-pythia8/RunIIFall17NanoAODv7-PU2017_12Apr2018_Nano02Apr2020_EXT_102X_mc2017_realistic_v8-v1/NANOAODSIM
/ZZZ_TuneCP5_13TeV-amcatnlo-pythia8/RunIIFall17NanoAODv7-PU2017_12Apr2018_Nano02Apr2020_EXT_102X_mc2017_realistic_v8-v1/NANOAODSIM
/ttZJets_TuneCP5_13TeV_madgraphMLM_pythia8/RunIIFall17NanoAODv7-PU2017_12Apr2018_Nano02Apr2020_102X_mc2017_realistic_v8_ext1-v1/NANOAODSIM
/ttZJets_TuneCP5_13TeV_madgraphMLM_pythia8/RunIIFall17NanoAODv7-PU2017_12Apr2018_Nano02Apr2020_102X_mc2017_realistic_v8-v1/NANOAODSIM
/ttWJets_TuneCP5_13TeV_madgraphMLM_pythia8/RunIIFall17NanoAODv7-PU2017_12Apr2018_Nano02Apr2020_102X_mc2017_realistic_v8_ext1-v1/NANOAODSIM
/ttWJets_TuneCP5_13TeV_madgraphMLM_pythia8/RunIIFall17NanoAODv7-PU2017_12Apr2018_Nano02Apr2020_102X_mc2017_realistic_v8-v1/NANOAODSIM
/GluGluToContinToZZTo2e2mu_13TeV_MCFM701_pythia8/RunIIFall17NanoAODv7-PU2017_12Apr2018_Nano02Apr2020_102X_mc2017_realistic_v8_ext1-v1/NANOAODSIM
/GluGluToContinToZZTo2e2mu_13TeV_MCFM701_pythia8/RunIIFall17NanoAODv7-PU2017_12Apr2018_Nano02Apr2020_EXT1_102X_mc2017_realistic_v8-v1/NANOAODSIM
/GluGluToContinToZZTo2e2tau_13TeV_MCFM701_pythia8/RunIIFall17NanoAODv7-PU2017_12Apr2018_Nano02Apr2020_102X_mc2017_realistic_v8_ext1-v1/NANOAODSIM
/GluGluToContinToZZTo2e2tau_13TeV_MCFM701_pythia8/RunIIFall17NanoAODv7-PU2017_12Apr2018_Nano02Apr2020_EXT1_102X_mc2017_realistic_v8-v1/NANOAODSIM
/GluGluToContinToZZTo2mu2tau_13TeV_MCFM701_pythia8/RunIIFall17NanoAODv7-PU2017_12Apr2018_Nano02Apr2020_102X_mc2017_realistic_v8_ext1-v1/NANOAODSIM
/GluGluToContinToZZTo2mu2tau_13TeV_MCFM701_pythia8/RunIIFall17NanoAODv7-PU2017_12Apr2018_Nano02Apr2020_EXT1_102X_mc2017_realistic_v8-v1/NANOAODSIM
/GluGluToContinToZZTo4e_13TeV_MCFM701_pythia8/RunIIFall17NanoAODv7-PU2017_12Apr2018_Nano02Apr2020_102X_mc2017_realistic_v8_ext1-v1/NANOAODSIM
/GluGluToContinToZZTo4e_13TeV_MCFM701_pythia8/RunIIFall17NanoAODv7-PU2017_12Apr2018_Nano02Apr2020_102X_mc2017_realistic_v8_ext2-v1/NANOAODSIM
/GluGluToContinToZZTo4e_13TeV_MCFM701_pythia8/RunIIFall17NanoAODv7-PU2017_12Apr2018_Nano02Apr2020_EXT_102X_mc2017_realistic_v8-v1/NANOAODSIM
/GluGluToContinToZZTo4mu_13TeV_MCFM701_pythia8/RunIIFall17NanoAODv7-PU2017_12Apr2018_Nano02Apr2020_102X_mc2017_realistic_v8_ext1-v1/NANOAODSIM
/GluGluToContinToZZTo4mu_13TeV_MCFM701_pythia8/RunIIFall17NanoAODv7-PU2017_12Apr2018_Nano02Apr2020_102X_mc2017_realistic_v8_ext2-v1/NANOAODSIM
/GluGluToContinToZZTo4mu_13TeV_MCFM701_pythia8/RunIIFall17NanoAODv7-PU2017_12Apr2018_Nano02Apr2020_EXT_102X_mc2017_realistic_v8-v1/NANOAODSIM
/GluGluToContinToZZTo4tau_13TeV_MCFM701_pythia8/RunIIFall17NanoAODv7-PU2017_12Apr2018_Nano02Apr2020_102X_mc2017_realistic_v8_ext1-v1/NANOAODSIM
/GluGluToContinToZZTo4tau_13TeV_MCFM701_pythia8/RunIIFall17NanoAODv7-PU2017_12Apr2018_Nano02Apr2020_102X_mc2017_realistic_v8-v1/NANOAODSIM
/GluGluZH_HToWW_M125_13TeV_powheg_pythia8_TuneCP5/RunIIFall17NanoAODv7-PU2017_12Apr2018_Nano02Apr2020_102X_mc2017_realistic_v8-v1/NANOAODSIM
/HZJ_HToWW_M125_13TeV_powheg_jhugen714_pythia8_TuneCP5/RunIIFall17NanoAODv7-PU2017_12Apr2018_Nano02Apr2020_102X_mc2017_realistic_v8-v1/NANOAODSIM
/ZZTo4L_13TeV_powheg_pythia8/RunIIFall17NanoAODv7-PU2017_12Apr2018_Nano02Apr2020_102X_mc2017_realistic_v8_ext1-v1/NANOAODSIM
/ZZTo4L_13TeV_powheg_pythia8/RunIIFall17NanoAODv7-PU2017_12Apr2018_Nano02Apr2020_102X_mc2017_realistic_v8_ext2-v1/NANOAODSIM
/ZZTo4L_13TeV_powheg_pythia8/RunIIFall17NanoAODv7-PU2017_12Apr2018_Nano02Apr2020_new_pmx_102X_mc2017_realistic_v8-v1/NANOAODSIM
/HWminusJ_HToWW_M125_13TeV_powheg_pythia8_TuneCP5/RunIIFall17NanoAODv7-PU2017_12Apr2018_Nano02Apr2020_102X_mc2017_realistic_v8-v1/NANOAODSIM
/HWplusJ_HToWW_M125_13TeV_powheg_pythia8_TuneCP5/RunIIFall17NanoAODv7-PU2017_12Apr2018_Nano02Apr2020_102X_mc2017_realistic_v8-v1/NANOAODSIM
/ggZH_HToTauTau_ZToLL_M125_13TeV_powheg_pythia8/RunIIFall17NanoAODv7-PU2017_12Apr2018_Nano02Apr2020_102X_mc2017_realistic_v8-v1/NANOAODSIM
/ggZH_HToTauTau_ZToNuNu_M125_13TeV_powheg_pythia8/RunIIFall17NanoAODv7-PU2017_12Apr2018_Nano02Apr2020_102X_mc2017_realistic_v8-v1/NANOAODSIM
/ggZH_HToTauTau_ZToQQ_M125_13TeV_powheg_pythia8/RunIIFall17NanoAODv7-PU2017_12Apr2018_Nano02Apr2020_102X_mc2017_realistic_v8-v1/NANOAODSIM
/ZHToTauTau_M125_13TeV_powheg_pythia8/RunIIFall17NanoAODv7-PU2017_12Apr2018_Nano02Apr2020_102X_mc2017_realistic_v8-v1/NANOAODSIM
/WminusHToTauTau_M125_13TeV_powheg_pythia8/RunIIFall17NanoAODv7-PU2017_12Apr2018_Nano02Apr2020_102X_mc2017_realistic_v8-v1/NANOAODSIM
/WplusHToTauTau_M125_13TeV_powheg_pythia8/RunIIFall17NanoAODv7-PU2017_12Apr2018_Nano02Apr2020_102X_mc2017_realistic_v8-v1/NANOAODSIM
/eos/home-s/shigginb/HAA_ntuples/ggha01a01Tomumutautau_2017_M15/
/eos/home-s/shigginb/HAA_ntuples/ggha01a01Tomumutautau_2017_M20/
/eos/home-s/shigginb/HAA_ntuples/ggha01a01Tomumutautau_2017_M25/
/eos/home-s/shigginb/HAA_ntuples/ggha01a01Tomumutautau_2017_M30/
/eos/home-s/shigginb/HAA_ntuples/ggha01a01Tomumutautau_2017_M35/
/eos/home-s/shigginb/HAA_ntuples/ggha01a01Tomumutautau_2017_M40/
/eos/home-s/shigginb/HAA_ntuples/ggha01a01Tomumutautau_2017_M45/
/eos/home-s/shigginb/HAA_ntuples/ggha01a01Tomumutautau_2017_M50/
/eos/home-s/shigginb/HAA_ntuples/ggha01a01Tomumutautau_2017_M55/
/eos/home-s/shigginb/HAA_ntuples/ggha01a01Tomumutautau_2017_M60/

Table 11: List of data sets included in the analysis for the 2018 data taking period.

Monte Carlo Datasets for 2018
/DY1JetsToLL_M-50_TuneCP5_13TeV-madgraphMLM-pythia8/RunIIAutumn18NanoAODv7-Nano02Apr2020_102X_upgrade2018_realistic_v21-v1/NANOAODSIM
/DY2JetsToLL_M-50_TuneCP5_13TeV-madgraphMLM-pythia8/RunIIAutumn18NanoAODv7-Nano02Apr2020_102X_upgrade2018_realistic_v21-v1/NANOAODSIM
/DY3JetsToLL_M-50_TuneCP5_13TeV-madgraphMLM-pythia8/RunIIAutumn18NanoAODv7-Nano02Apr2020_102X_upgrade2018_realistic_v21-v1/NANOAODSIM
/DY4JetsToLL_M-50_TuneCP5_13TeV-madgraphMLM-pythia8/RunIIAutumn18NanoAODv7-Nano02Apr2020_102X_upgrade2018_realistic_v21-v1/NANOAODSIM
/DYJetsToLL_M-50_TuneCP5_13TeV-madgraphMLM-pythia8/RunIIAutumn18NanoAODv7-Nano02Apr2020_102X_upgrade2018_realistic_v21-v1/NANOAODSIM
/DYJetsToLL_M-10to50_TuneCP5_13TeV-madgraphMLM-pythia8/RunIIAutumn18NanoAODv7-Nano02Apr2020_102X_upgrade2018_realistic_v21-v1/NANOAODSIM
/DYJetsToLL_M-10to50_TuneCP5_13TeV-madgraphMLM-pythia8/RunIIAutumn18NanoAODv7-Nano02Apr2020_102X_upgrade2018_realistic_v21_ext1-v1/NANOAODSIM
/W1JetsToLNu_TuneCP5_13TeV-madgraphMLM-pythia8/RunIIAutumn18NanoAODv7-Nano02Apr2020_102X_upgrade2018_realistic_v21-v1/NANOAODSIM
/W2JetsToLNu_TuneCP5_13TeV-madgraphMLM-pythia8/RunIIAutumn18NanoAODv7-Nano02Apr2020_102X_upgrade2018_realistic_v21-v1/NANOAODSIM
/W3JetsToLNu_TuneCP5_13TeV-madgraphMLM-pythia8/RunIIAutumn18NanoAODv7-Nano02Apr2020_102X_upgrade2018_realistic_v21-v1/NANOAODSIM
/W4JetsToLNu_TuneCP5_13TeV-madgraphMLM-pythia8/RunIIAutumn18NanoAODv7-Nano02Apr2020_102X_upgrade2018_realistic_v21-v1/NANOAODSIM
/WJetsToLNu_TuneCP5_13TeV-madgraphMLM-pythia8/RunIIAutumn18NanoAODv7-Nano02Apr2020_102X_upgrade2018_realistic_v21-v1/NANOAODSIM
/WZTo3LNu_TuneCP5_13TeV-powheg-pythia8/RunIIAutumn18NanoAODv7-Nano02Apr2020_102X_upgrade2018_realistic_v21_ext1-v1/NANOAODSIM
/WWW_4F_TuneCP5_13TeV-amcatnlo-pythia8/RunIIAutumn18NanoAODv7-Nano02Apr2020_102X_upgrade2018_realistic_v21_ext1-v1/NANOAODSIM
/WWZ_TuneCP5_13TeV-amcatnlo-pythia8/RunIIAutumn18NanoAODv7-Nano02Apr2020_102X_upgrade2018_realistic_v21_ext1-v1/NANOAODSIM
/WZZ_TuneCP5_13TeV-amcatnlo-pythia8/RunIIAutumn18NanoAODv7-Nano02Apr2020_102X_upgrade2018_realistic_v21_ext1-v1/NANOAODSIM
/ZZZ_TuneCP5_13TeV-amcatnlo-pythia8/RunIIAutumn18NanoAODv7-Nano02Apr2020_102X_upgrade2018_realistic_v21_ext1-v1/NANOAODSIM
/ttZJets_TuneCP5_13TeV_madgraphMLM_pythia8/RunIIAutumn18NanoAODv7-Nano02Apr2020_102X_upgrade2018_realistic_v21_ext1-v1/NANOAODSIM
/ttWJets_TuneCP5_13TeV_madgraphMLM_pythia8/RunIIAutumn18NanoAODv7-Nano02Apr2020_102X_upgrade2018_realistic_v21_ext1-v1/NANOAODSIM
/GluGluHToTauTau_M125_13TeV_powheg_pythia8/RunIIAutumn18NanoAODv7-Nano02Apr2020_102X_upgrade2018_realistic_v21-v1/NANOAODSIM
/GluGluToContinToZZTo2e2mu_13TeV_TuneCP5_MCFM701_pythia8/RunIIAutumn18NanoAODv7-Nano02Apr2020_102X_upgrade2018_realistic_v21-v1/NANOAODSIM
/GluGluToContinToZZTo2e2tau_13TeV_TuneCP5_MCFM701_pythia8/RunIIAutumn18NanoAODv7-Nano02Apr2020_102X_upgrade2018_realistic_v21-v1/NANOAODSIM
/GluGluToContinToZZTo2mu2tau_13TeV_MCFM701_pythia8/RunIIAutumn18NanoAODv7-Nano02Apr2020_102X_upgrade2018_realistic_v21-v1/NANOAODSIM
/GluGluToContinToZZTo4e_13TeV_MCFM701_pythia8/RunIIAutumn18NanoAODv7-Nano02Apr2020_102X_upgrade2018_realistic_v21_ext1-v1/NANOAODSIM
/GluGluToContinToZZTo4e_13TeV_MCFM701_pythia8/RunIIAutumn18NanoAODv7-Nano02Apr2020_EXT_102X_upgrade2018_realistic_v21-v1/NANOAODSIM
/GluGluToContinToZZTo4mu_13TeV_MCFM701_pythia8/RunIIAutumn18NanoAODv7-Nano02Apr2020_102X_upgrade2018_realistic_v21_ext1-v1/NANOAODSIM
/GluGluToContinToZZTo4mu_13TeV_MCFM701_pythia8/RunIIAutumn18NanoAODv7-Nano02Apr2020_EXT_102X_upgrade2018_realistic_v21-v1/NANOAODSIM
/GluGluToContinToZZTo4tau_13TeV_MCFM701_pythia8/RunIIAutumn18NanoAODv7-Nano02Apr2020_EXT_102X_upgrade2018_realistic_v21-v1/NANOAODSIM
/HZJ_HToWW_M125_13TeV_powheg_jhugen714_pythia8_TuneCP5/RunIIAutumn18NanoAODv7-Nano02Apr2020_102X_upgrade2018_realistic_v21-v1/NANOAODSIM
/ZZTo4L_TuneCP5_13TeV_powheg_pythia8/RunIIAutumn18NanoAODv7-Nano02Apr2020_102X_upgrade2018_realistic_v21_ext1-v1/NANOAODSIM
/ZZTo4L_TuneCP5_13TeV_powheg_pythia8/RunIIAutumn18NanoAODv7-Nano02Apr2020_102X_upgrade2018_realistic_v21_ext2-v1/NANOAODSIM
/ZZTo4L_13TeV_powheg_pythia8_TuneCP5/RunIIAutumn18NanoAODv7-Nano02Apr2020_102X_upgrade2018_realistic_v21-v1/NANOAODSIM
/ggZH_HToTauTau_ZToLL_M125_13TeV_powheg_pythia8/RunIIAutumn18NanoAODv7-Nano02Apr2020_102X_upgrade2018_realistic_v21-v1/NANOAODSIM
/ggZH_HToTauTau_ZToNuNu_M125_13TeV_powheg_pythia8/RunIIAutumn18NanoAODv7-Nano02Apr2020_102X_upgrade2018_realistic_v21-v1/NANOAODSIM
/ggZH_HToTauTau_ZToQQ_M125_13TeV_powheg_pythia8/RunIIAutumn18NanoAODv7-Nano02Apr2020_102X_upgrade2018_realistic_v21-v1/NANOAODSIM
/GluGluZH_HToWW_M125_13TeV_powheg_pythia8_TuneCP5_PSweights/RunIIAutumn18NanoAODv7-Nano02Apr2020_102X_upgrade2018_realistic_v21-v1/NANOAODSIM
/WminusHToTauTau_M125_13TeV_powheg_pythia8/RunIIAutumn18NanoAODv7-Nano02Apr2020_102X_upgrade2018_realistic_v21-v1/NANOAODSIM
/WplusHToTauTau_M125_13TeV_powheg_pythia8/RunIIAutumn18NanoAODv7-Nano02Apr2020_102X_upgrade2018_realistic_v21-v1/NANOAODSIM
/ZHToTauTau_M125_13TeV_powheg_pythia8/RunIIAutumn18NanoAODv7-Nano02Apr2020_102X_upgrade2018_realistic_v21-v1/NANOAODSIM
/HWminusJ_HToWW_M125_13TeV_powheg_jhugen724_pythia8_TuneCP5/RunIIAutumn18NanoAODv7-Nano02Apr2020_102X_upgrade2018_realistic_v21-v1/NANOAODSIM
/HWplusJ_HToWW_M125_13TeV_powheg_jhugen724_pythia8_TuneCP5/RunIIAutumn18NanoAODv7-Nano02Apr2020_102X_upgrade2018_realistic_v21-v1/NANOAODSIM
/eos/home-s/shigginb/HAA_ntuples/ggha01a01Tomumutautau_2018_dtau_M15/
/eos/home-s/shigginb/HAA_ntuples/ggha01a01Tomumutautau_2018_dtau_M20/
/eos/home-s/shigginb/HAA_ntuples/ggha01a01Tomumutautau_2018_dtau_M25/
/eos/home-s/shigginb/HAA_ntuples/ggha01a01Tomumutautau_2018_dtau_M30/
/eos/home-s/shigginb/HAA_ntuples/ggha01a01Tomumutautau_2018_dtau_M35/
/eos/home-s/shigginb/HAA_ntuples/ggha01a01Tomumutautau_2018_dtau_M40/
/eos/home-s/shigginb/HAA_ntuples/ggha01a01Tomumutautau_2018_dtau_M45/
/eos/home-s/shigginb/HAA_ntuples/ggha01a01Tomumutautau_2018_dtau_M50/
/eos/home-s/shigginb/HAA_ntuples/ggha01a01Tomumutautau_2018_dtau_M55/
/eos/home-s/shigginb/HAA_ntuples/ggha01a01Tomumutautau_2018_dtau_M60/

References

[1] F. Englert and R. Brout, "Broken symmetry and the mass of gauge vector mesons", *Phys. Rev. Lett.* **13** (1964) 321, doi:10.1103/PhysRevLett.13.321.

[2] P. W. Higgs, "Broken symmetries, massless particles and gauge fields", *Phys. Lett.* **12** (1964) 132, doi:10.1016/0031-9163(64)91136-9.

[3] P. W. Higgs, "Broken symmetries and the masses of gauge bosons", *Phys. Rev. Lett.* **13** (1964) 508, doi:10.1103/PhysRevLett.13.508.

[4] G. S. Guralnik, C. R. Hagen, and T. W. B. Kibble, "Global conservation laws and massless particles", *Phys. Rev. Lett.* **13** (1964) 585, doi:10.1103/PhysRevLett.13.585.

[5] P. W. Higgs, "Spontaneous symmetry breakdown without massless bosons", *Phys. Rev.* **145** (1966) 1156, doi:10.1103/PhysRev.145.1156.

[6] T. W. B. Kibble, "Symmetry Breaking in Non-Abelian Gauge Theories", *Phys. Rev.* **155** (1967) 1554, doi:10.1103/PhysRev.155.1554.

[7] CMS Collaboration, "Search for an exotic decay of the higgs boson to a pair of light pseudoscalars in the final state of two muons and two τ leptons in proton-proton collisions at $\sqrt{s} = 13$tev leptons with the CMS detector", *Journal of High Energy Physics* (2017) 283, doi:10.1007/JHEP11(2018)018, arXiv:1805.04865.

[8] G. Branco et al., "Theory and phenomenology of two-higgs-doublet models", *Physics Reports* **516** (jul, 2012) 1–102, doi:10.1016/j.physrep.2012.02.002.

[9] CMS Collaboration, "The CMS trigger system", *JINST* **12** (2017) P01020, doi:10.1088/1748-0221/12/01/P01020, arXiv:1609.02366.

[10] CMS Collaboration, "The CMS experiment at the CERN LHC", *JINST* **03** (2008) S08004, doi:10.1088/1748-0221/3/08/S08004.

[11] T. Sjostrand, S. Mrenna, and P. Z. Skands, "PYTHIA 6.4 Physics and Manual", *JHEP* **0605** (2006) 026, doi:10.1088/1126-6708/2006/05/026, arXiv:hep-ph/0603175.

[12] GEANT4 Collaboration, "GEANT4: A simulation toolkit", *Nucl. Instrum. Meth. A* **506** (2003) 250, doi:10.1016/S0168-9002(03)01368-8.

[13] CMS Collaboration, "Measurements of higgs boson production in the decay channel with a pair of τ leptons in proton-proton collisions at $\sqrt{s}$ = 13 tev", 2022. doi:10.48550/ARXIV.2204.12957, https://arxiv.org/abs/2204.12957.

[14] CMS Collaboration Collaboration, "Measurement of Higgs boson production in the decay channel with a pair of τ leptons", technical report, CERN, Geneva, 2020.

[15] G. Cowan, K. Cranmer, E. Gross, and O. Vitells, "Asymptotic formulae for likelihood-based tests of new physics", *The European Physical Journal C* **71** (feb, 2011) doi:10.1140/epjc/s10052-011-1554-0.